ELSEVIER

Journal of Chromatography A, 798 (1998) 223–232

JOURNAL OF CHROMATOGRAPHY A

Isotachophoretic focusing of strong electrolytes on the background of carrier ampholytes

Tomáš Rejtar, Karel Šlais*

Institute of Analytical Chemistry, Academy of Sciences of the Czech Republic, Veveří 97, 611 42 Brno, Czech Republic

Abstract

In this contribution, the predicted possibility of separation and focusing of strong electrolytes in a conductivity gradient was verified. Homologous series of derivatized polyethylene glycols and oligomaltoses were separated and focused in combined pH and conductivity gradient generated by isotachophoretic moving of a stack of carrier polyampholytes. Since the chosen analytes were anions of sulfonic acids, the influence of pH gradient on analyte mobility could be neglected. The experimentally found peak widths and resolutions were comparable with calculated ones. The dependencies of the peak resolution on the composition of leading and terminating electrolytes as well as on the amount of carrier ampholytes and the electric current were studied. © 1998 Elsevier Science B.V.

Keywords: Isotachophoretic focusing; Buffer composition; Conductivity gradients; Poly(ethylene glycol); Oligomaltoses

1. Introduction

Isotachophoresis (ITP) is an electrophoretic separation technique that is able to separate and focus strong, weak as well as ampholytic analytes. Due to its high separation power, it is used both in analytical practice and for preparative purposes [1,2]. Under the steady state, the analytes are focused into adjacent square-wave zones. The evaluation of the detection record is therefore more difficult in comparison with separated Gaussian zones which are common, e.g., in zone electrophoresis and chromatography. This disadvantage can be eliminated by several approaches: (i) by use of discrete spacers with suitable detector response which are focused between the zones of analytes [3,4]; (ii) by coupling of ITP with capillary zone electrophoresis (CZE) [5] (in this mode, the square-wave ITP zones are separated on-line into the Gaussian shape peaks by CZE); (iii) by use of carrier electrolytes, e.g., polyampholytes. In the carrier polyampholyte background, the ampholytes are focused into the Gaussian peaks which are included in the stack of ordered and focused background components. This type of separation was used by Mikkers ([1] pp. 322–336) for the analysis of proteins. Such an electrophoretic separation mode is called either isotachophoresis with carrier ampholytes [6–10], capillary isoelectric focusing (IEF) with electrophoretic mobilization [11,12], isotachophoresis–isoelectrofocusing [13] or isotachophoretic focusing (ITF) [14,15]. In most of the references, an approximately linear pH gradient is considered and the separation mechanism is supposed to be similar to that of IEF. Nevertheless, the gradient of field strength and thus the gradient of conductivity occurs in the isotachophoretically moving stack of carrier ampholytes [1,6]. Charlionet et al. [14,15] published equations for the description of the behavior of ampholytes in the conductivity gradient without consideration of the pH. The sepa-

*Corresponding author. Fax: +420-5-41212113.

0021-9673/98/$19.00
PII S0021-9673(97)00996-5

ration and focusing of nucleotides in combined conductivity and very shallow pH gradient was demonstrated [6]. Since the nucleotides behave as strong electrolytes under conditions used, their separation cannot be explained by focusing in the pH gradient. Thus, their separation occurs due to the present conductivity gradient.

A recently published theory [16] describes focusing of both weak and strong electrolytes in pH and conductivity gradients. The aim of this paper is to verify the predicted features of separation and focusing of strong electrolytes in a conductivity gradient. Homologous series of UV-detectable hydrophilic strong analytes were separated and focused in the combined pH and conductivity gradient generated by isotachophoretic moving of carrier polyampholytes. Since the chosen analytes are anions of sulfonic acids, the influence of the pH gradient on analyte mobility can be neglected. The dependence of the composition of leading and terminating electrolytes on the separation was studied. Further, the influence of the amount of carrier ampholytes and the electric current were demonstrated.

2. Theory

A model of focusing and separation of charged compounds in a gradient of conductivity was presented previously [16]. The principle of the method is outlined in Fig. 1. Prior to the analysis, the separation compartment is filled by a leading electrolyte, LE; the carriers, CA, and sample, S, are injected between the LE and the terminating electrolyte, TE, see Fig. 1a. After switching the current on, all anions move to the detection end of the capillary and are ordered according to their effective mobilities, see Fig. 1b. In this way, the conductivity gradient is formed from a great number of good ampholytes which are focused into the Gaussian shape peaks under isotachophoretic conditions, see Fig. 1c. This conductivity gradient is considered as continuous and the analytes are focused and separated on its background. Though it should be kept in mind that gradient steepness and shape depends on the composition of leading and terminating electrolytes, the linear gradient can be considered when

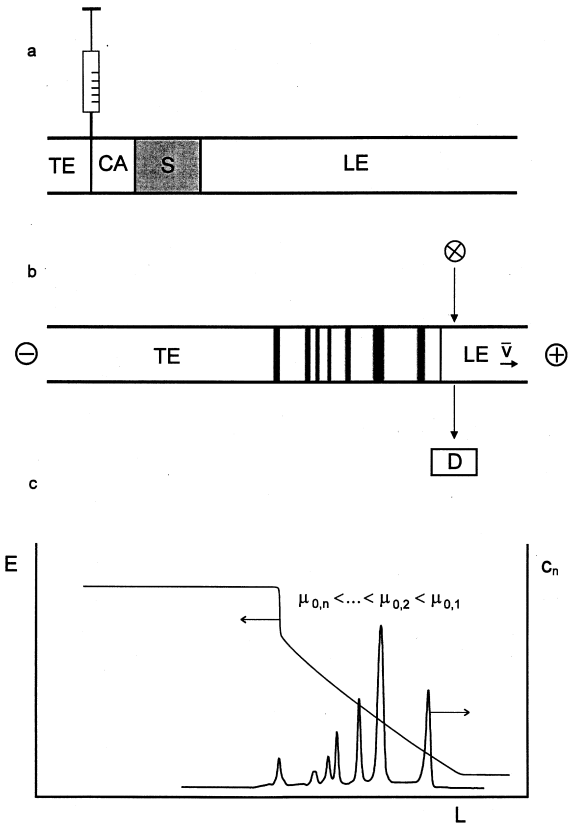

Fig. 1. Illustration of the separation principle. a: electrolyte design after the injection; b: electrolyte design in the steady state; c: gradient of field strength and concentration of focused analytes. Symbols: TE: terminating electrolyte, CA: carrier ampholytes, S: sample, LE: leading electrolyte, $\bar{v}$: isotachophoretic velocity, D: detector, E: field strength, c_n: concentration of analytes, L: separation distance, $\mu_{0,n}$: mobilities of analytes.

discussing the peak shape and resolution of closely separated peaks [17].

For the zone of the analyte in the steady state, the peak variance, σ_x^2, can be expressed in the following way [16]:

$$\sigma_x^2 = \frac{-D}{\frac{d\mu}{dx}E + \bar{\nu}\frac{d \ln \rho}{dx}} \quad (1)$$

where D is a diffusion coefficient of analyte, E is electric field strength, $\bar{v}$ is isotachophoretic velocity, ρ is resistivity ($\rho = 1/\kappa$, where κ is conductivity), μ is analyte effective mobility and x is the length

coordinate along the moving gradient with $x=0$ at the peak maximum. The derivation $d\rho/dx$ represents the steepness of the resistivity gradient along the zone. This is a general equation considering the influence of both resistivity and pH gradients. For strong electrolytes which do not change their mobility with pH (and $d\mu/dx=0$), it follows from Eq. (1), according to [16]:

$$\sigma_x^2 = \frac{D}{\frac{\bar{\mu} I}{A}\frac{-d\rho}{dx}} \quad (2)$$

where I is electric current and A is cross section. By insertion of the Nernst–Einstein equation:

$$\mu = \frac{zFD}{RT} \quad (3)$$

into Eq. (2), the following equation can be derived, see [16]:

$$\sigma_x^2 = \frac{RT}{\frac{zFI}{A}\frac{-d\rho}{dx}} \quad (4)$$

where z is an effective electric charge of analyte. For monoprotic strong anionic electrolytes, it is $z=-1$. Symbols R, T and F have usual meaning. After rearrangement of Eq. (4), the final form suitable for the calculation of peak variance from detector record is obtained.

$$\sigma_x^2 = \frac{RT}{\frac{zF}{\mu}\left(\frac{1}{\mu}\frac{d\mu}{dt}\right)} \quad (5)$$

where $d\mu/dt$ is the time change of the mobility which would be monitored at the detector position. When the analytes are strong electrolytes, this quantity can be approximated from differences in their known ionic mobilities and measured migration times.

For expression of peak variance in the time units, Eq. (6) is used:

$$\sigma_t = \frac{\sigma_x}{\bar{\nu}} \quad (6)$$

Further, final form of the equation for theoretical resolution between peaks n and $n+1$ can be derived [16]:

$$R_s(n,n+1) = \frac{\mu_n - \mu_{n+1}}{4\bar{\mu}}\sqrt{\frac{F\bar{\nu}^2}{RT\frac{d\mu}{dt}}} \quad (7)$$

where the term in front of the root represents selectivity similarly as in CZE.

In order to compare the theoretical peak variances with the experimental ones it is necessary to correct the theoretical values for σ_t the detector time constant and for the light beam diameter [18,32]. The corrected peak variance σ_{cor} is then calculated as a root of sum of the squares of all contributions.

Since Eq. (7) does not allow the inclusion of the above described corrections, the corrected resolution will be calculated according to the following equation:

$$R_s(n,n+1)_{cor} = \frac{t_{n+1} - t_n}{2(\sigma_{cor}(n) + \sigma_{cor}(n+1))} \quad (8)$$

3. Experimental

3.1. Equipment

All of the experiments were carried out on the automated miniaturized instrument which has been described previously [18,19]. The instrument consists of the liquid handling device controlled by a microprocessor and the separation compartment with the detection system. The separation channel had a tapered shape with inner diameter decreasing from 0.8 to 0.4 mm, length 9 mm and total volume 3 μl. This tapered shape was used to decrease the total applied voltage [18–21]. The fused-silica capillary with 0.25 mm inner diameter and length 5 cm, was used for detection. The 5-cm long capillary of 0.32 mm I.D. was inserted between the tapered channel and the detection capillary in order to increase the total volume of the separation compartment. The on column UV–Vis detector LCD 2082 (Ecom, Prague, Czech Republic) was connected to the detection capillary by optical fibers [22]. The analytical signal was collected by personal computer equipped with CSW data handling software (DataApex, Prague, Czech Republic). A line recorder TZ 4620 (Laboratory Instruments, Prague, Czech Republic) was used for registration of the total voltage along the separation compartment.

3.2. Chemicals

All chemicals were analytical grade. Picric acid, 4-hydroxy-3-nitrobenzoic acid, poly(ethylene glycol) (PEG) $M_r = 200$ and 400 g/mol, 1-amino-4-naphthalenesulfonic acid (ANSA), β-cyclodextrin hydrate (β-CD) and mesityl oxide were obtained from Aldrich (Milwaukee, WI, USA); tris(hydoxymethyl)aminomethane (Tris), 2-sulfobenzoic acid cyclic anhydride, methyl orange, sodium hydroxide and cetyltrimethylammonium bromide (CTAB) from Lachema (Brno, Czech Republic), 2-hydroxyisobutyric acid (HIBA) and phenol red from Fluka (Switzerland), hydroxypropylmethyl cellulose (HPMC), 2-amino-2-methyl-1-propanol (AMP) and sodium cyanoborohydride from Sigma (St. Louis, MO, USA), tris(hydoxymethyl)aminomethane hydrochloride (Tris·HCl), 2-(cyclohexylamino)ethanesulfonic acid (CHES) and 3-morpholinopropanesulfonic acid (MOPS) from Merck (Darmstadt, Germany), polyethylenimine (PEI) from Serva (Heidelberg, Germany).

The low-molecular-mass colored ampholytes (p*I* markers) 2,6-bis[(4-methyl-1-piperazinyl)methyl]-4-nitrophenol [95380-45-3] (3) and 2-(4-morpholinylmethyl)-4-nitrophenol [69245-0] (15) were prepared in the Institute of Analytical Chemistry (Academy of Sciences, Brno, Czech Republic). The number of p*I* markers in the squared brackets were taken from Chemical Abstracts (CA registry numbers) and the numbers in brackets are according to [23,24].

The solution of synthetic carrier ampholyte Ampholine pH 3.5–10.0 was purchased from Pharmacia LKB (Uppsala, Sweden).

3.3. Electrolyte system

A solution of 10 m*M* HIBA (leader) and 11 m*M* Tris (counterion) was used in most of the cases as the leading electrolyte (LE). The pH of the leading electrolyte was varied from 6.6 to 9.2 by changing the concentration of Tris. In some of the experiments, the system chloride/Tris (leader/counterions) was used. As the terminating electrolytes solution of AMP or mixture of CHES and NaOH were used.

All of the experiments were carried out in the closed mode of ITP and due to this the modification of the fused-silica inner wall and the control of electrosmosis were necessary [25–27]. The dynamic coating of detection capillary by adding HPMC and PEI [28] into the leading electrolyte was chosen. The 1–8% (v/v) solution of Ampholine was used as carrier ampholyte.

3.4. Preparation of model analytes

Esterification reaction of polyethylene glycol was performed by mixing 1.0 g of PEG with 0.1 g of 2-sulfobenzoic acid cyclic anhydride. This mixture was incubated for 7 h at 100°C. For analysis, a hundred times diluted solution was used.

Aminonaphtalenesulfonic acid derivatization reaction of oligomaltoses was performed by adaptation of the Jackson's method [29,30]. The mixture of oligomaltoses was prepared by hydrolysis of β-CD by HCl: 50 mg of β-CD, 10 μl concentrated HCl and 0.1 ml of water was incubated for 3 h at 80°C. The derivatization was done by the following procedure: 1 mg of ANSA, 20 μl of concentrated acetic acid and 50 μl of hydrolyzed β-CD were dissolved in 1 ml of water. This mixture was incubated for 1.5 h at 80°C and then 5 mg of sodium cyanoborohydride was added and again heated for 1 h at 80°C. For the analysis, ten times diluted solution was used. The derivatized oligomaltoses were stored at −18°C and kept at room temperature as little as possible.

3.5. Measurement of the model analytes mobilities

The preparation of the model analytes was described in Section 3.4. Since only some of the mobilities of these compounds are available from the literature, they had to be measured. The CZE electrophoretic mode with 200 μm I.D. fused-silica capillary was chosen. The total length of the capillary was 47 cm (32 cm to the detection). The UV detector Jasco 970 (Jasco, Tokyo, Japan) and high power supplier VN Spellman CZE 1000R (New York, USA) were used. The background electrolyte was composed of 10 m*M* MOPS and 7 m*M* Tris, pH = 7.3. Moreover 0.06% (w/v) HPMC and 0.2 m*M* CTAB were added into the background electrolyte to reduce the endoosmotic flow. Further 0.05% mesityl oxide was used as a marker of endoosmosis. The value of the measured mobilities of model analytes are in Table 1, third column.

Table 1
Calculation of theoretical peak variance and peak resolution. Comparison with experimental values

n[a]	t (min)	$-\mu$ (10^{-9} m^2 V^{-1} s^{-1})	$\Delta\mu/\Delta t$ (10^{-10} m^2 V^{-1} s^{-2})	σ_t (s)	σ_{cor} (s)	σ_{exp} (s)	$R_s(n,n+1)_{cor}$	$R_s(n,n+1)_{exp}$
Derivatized PEGs								
1	26.88	26.3	−0.867	4.14	4.28	2.88	2.26	3.14
2	27.49	23.1	−0.847	3.68	3.84	2.98	1.51	1.77
3	27.88	21.1	−0.710	3.68	3.83	3.57	1.75	1.34
4	28.27	19.4	−1.130	2.69	2.90	5.27	1.21	0.70
5	28.51	17.8	−0.853	2.83	3.03	5.02	1.32	1.11
6	28.80	16.4	−0.551	3.24	3.41	2.62	1.65	2.10
7	29.18	15.1	−0.445	3.33	3.50	2.22	–	1.52
Derivatized oligomaltoses								
0	25.99[b]	21.4	−0.246	6.34	6.43	5.78	7.49	6.98
1	28.50[b]	17.7	−0.566	3.45	3.62	5.02	3.49	2.84
2	29.38[b]	14.7	−0.329	3.77	3.92	4.26	4.29	3.01
3	30.32[b]	12.9	−0.585	2.47	2.69	5.17	1.98	1.15
4	30.70[b]	11.5	−0.380	2.75	2.95	4.59	2.14	1.53
5	31.13[b]	10.6	−0.287	2.89	3.09	3.82	–	1.52

[a] Number of monomers in oligomer. Reagent represents $n=0$.
[b] Migration times corrected for the presence of electrolytes. See Section 4.2.

3.6. Measurement of the linear velocity of moving stack

For computing the theoretical values of peak variances and resolution, it is necessary to know the linear ITP velocity of the moving stack. This velocity is a function of electrical current and composition of leading electrolyte. The leading electrolyte consisted of 10 m*M* HIBA, 12 m*M* Tris, 0.6% (w/v) HPMC and 5 μg/ml PEI. As a terminating electrolyte 0.1 *M* AMP was used. The electric current 12 μA was applied. The time in which the zone of 1.0 mg/ml concentrated phenol red travelled the 30-mm distance in the detection capillary was measured. Under the assumption that the zone is at the steady state, the linear velocity is equal to the ratio of the passed distance and the corresponding measured time.

4. Results and discussion

4.1. Minimization of endoosmotic flow

The modification of the inner fused-silica capillary wall and the control of endoosmotic flow was necessary because all experiments were done in the closed mode of ITP. Many experiments were performed in a longer time period and the covalent coating [31] of the fused-silica capillary would not ensure the required stability. That is why the dynamic coating of endoosmotic flow was chosen. It was done by adding HPMC and PEI into the leading electrolyte. The optimal HPMC concentration 0.06% (w/v) and PEI concentration 5 μg/ml were found for the mixture of 4-hydroxy-3-nitro-benzoic acid, picric acid, methyl orange, p*I* markers (3) and (15). The leading electrolyte consisted of 10 m*M* Tris·HCl, 10 m*M* Tris (pH=8.0) and additives. Terminating electrolyte was 0.1 *M* AMP, electric current 12 μA, $\lambda=400$ nm. As a background, 400 nl 1.4% ampholine was used.

4.2. Separation and focusing of model mixtures

Examples of separation and focusing of model mixtures are presented in Fig. 2a and b. The numbers of monomers in oligomers belonging to peaks in Fig. 2a and b and in Table 1 (symbol *n*) were obtained from experiments with first three monodisperse members of oligomeric series.

The electrolyte system was chosen to establish the conductivity gradient with shallow pH gradient. Since all of the model analytes were strong electrolytes, their migration can not be influenced by pH gradient; the separation takes place only by the

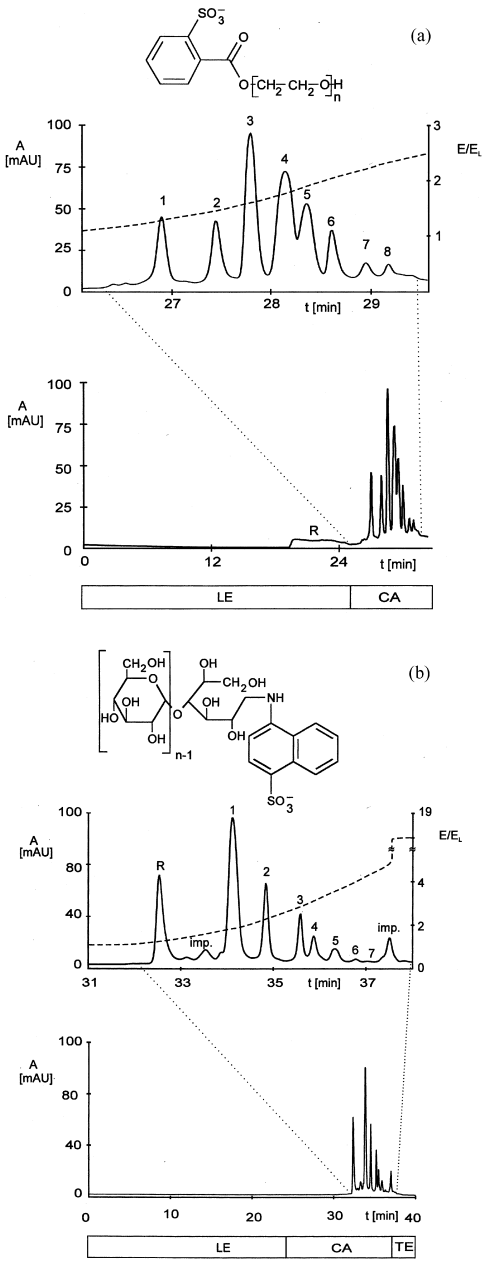

Fig. 2. Analysis of derivatized a: PEG, b: oligomaltoses. *R*: peak of reagent, numbers represent the *n* in the analyte formula structure. E/E_L is a ratio of field strength during analysis to the beginning of analysis. LE: leading electrolyte, CA: carrier ampholyte, TE: terminating electrolyte. Conditions: LE (pH=7.2) 10 m*M* HIBA, 11 m*M* Tris, 0.06% (w/v) HPMC, 5 μg/ml PEI; TE 50 m*M* CHES, 5 m*M* NaOH; background 4% Ampholine pH 3.5–10.0; sample volume 500 nl, background 400 nl; I=12 μA, in a λ=270 nm, in b λ=330 nm.

focusing in conductivity gradient. However, the composition and pH of leading electrolyte influence the process of establishing the conductivity profile. This is caused by the fact that carrier ampholytes are a non-homogenous mixture of ampholytes and the extent of their ionization depends on the pH of the leading electrolyte.

Since the conductivity gradient is related to mobilities of ordered stack components, the shape of conductivity profile can by visualized by Fig. 3, where the mobility profiles for several pH values of LE are plotted against the distance of a particular peak from the peak of reagent (1-amino-4-naphthalenesulfonic acid). It was found that for the lower value of pH of leading electrolyte (6.6–7.9) it is almost an exponential decrease of mobility in the gradient. This makes the conditions found, similar to the model [16] where resistivity linearly increases with separation distance. It means the inverse proportional decrease of mobility with separation distance. The dependence on a higher value of pH (8 and higher) shows the curvature in the range of lower

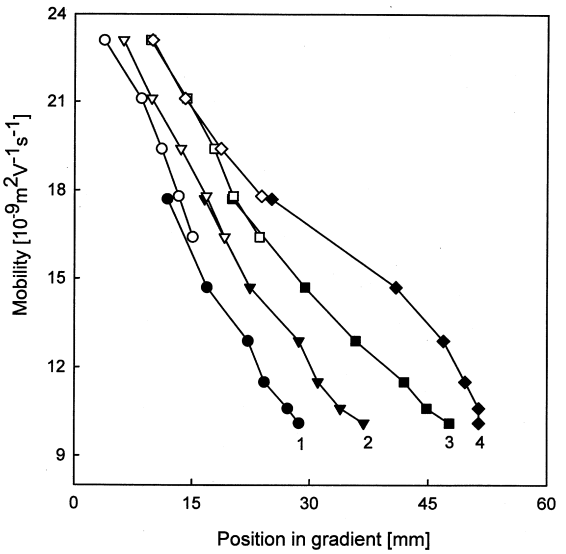

Fig. 3. Dependence of mobility in the gradient on the distance of peaks from the peak of reagent for various pH of leading electrolyte. Hollow symbols are for derivatized PEG, filled symbols for derivatized oligomaltoses. Conditions: leading electrolyte 10 m*M* HIBA and Tris pH: 1=6.62, 2=7.23, 3=7.90, 4=8.59. Other conditions as in Fig. 2a, b.

mobilities. This is probably caused by the lack of low mobility carrier ampholytes at higher pH values.

It was found that the observed conductivity gradient is not free from local fluctuations of the steepness, see curves in Fig. 3. The gradient is not smooth due to non-uniform distribution of components of carrier ampholytes. Also, the separation distance between the model analytes are not monotonously decreasing as it is supposed in the model. Of course, the carrier ampholytes were primarily developed and optimized for smooth pH gradient in IEF. Nevertheless, they are the only available compounds for generation of conductivity gradient in ITF now.

In Fig. 4, the dependence of the resolution of derivatized oligomaltoses on the pH of the leading electrolyte is shown. For the electrolyte system used, it is possible to change the pH approximately from 7 to 9. For a pH lower then 7, the overall resistance of the system is too big and for a pH higher then 9 the resolution decreases. The working pH range is restricted by pK_a of the counterion (Tris, pK_a = 8.07). The use of another counterion would enable work in another pH range. A not very apparent optimum at pH = 7.2 was chosen for further studies.

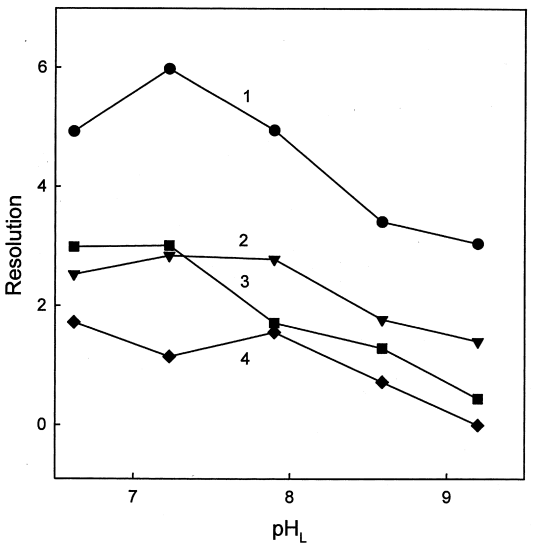

Fig. 4. Dependence of resolution on the pH of leading electrolyte. (1) = $R_{0,1}$, (2) = $R_{1,2}$, (3) = $R_{2,3}$ and (4) = $R_{3,4}$. Other conditions as in Fig. 3.

From the known conductivity gradient profile and Eqs. (5)–(7), it is possible to calculate the theoretical peak variance and resolution. The measurement of a moving stack linear velocity was described in Section 3.6 and the value 0.11 mm/s was found. The results are presented in Table 1. The presence of acetic acid and hydrochloric acid from the derivatizing procedure in the sampled solution of oligomaltoses makes the measured migration times longer because acetic acid and hydrochloric acid migrate as typical square wave ITP zones at the leading edge of the stack of carrier ampholytes. That is why the values of migration times found, presented in Table 1 and Fig. 2b, were shortened correspondingly. The measurement of mobilities of model analytes was described in Section 3.5. The $d\mu/dt$ term was approximated by three different ways of calculation: (i) as the ratio of differences of mobilities and separation times between neighboring zones of analytes (in this case, the value of derivatization does not exactly match the calculated point); (ii) from the differences between the lower and the higher neighbors of calculated peak and (iii) from derivatized regression of the dependence in Fig. 3. The differences in the calculated values of $\Delta\mu/\Delta t$ term between the above three approaches were lower than ±20%. For further calculation, the approach under (i) was chosen. The reproducibility of the mobility gradient was verified. The relative standard deviation of the term $\Delta\mu/\Delta t$ from four experiments was found to be 7%. This means that the reproducibility of the experiment is better than the error caused by the calculation of $\Delta\mu/\Delta t$ and that is why values from a single typical experiment were used for further calculation. The calculated σ_t values summarized in Table 1 were calculated from Eqs. (5) and (6). The theoretical peak variances σ_t were corrected (σ_{cor}) for the detection time constant (1 s) and for the light beam diameter (0.4 s) [18,32].

For derivatized PEG, the experimental peak variances, σ_{exp}, are smaller than the theoretical one, σ_{cor}, in some cases. This can be caused by local changes in steepness of gradient since the local increase in conductivity gradient can induce more significant focusing. For derivatized oligomaltoses, the experimental peak variances are comparable to the theoretical ones. In both homologous series, the tendency of decrease of peak variances with decrease

in the mobility can be seen which can be expected from the theory.

The sampled analyte is present in a volume of about 1 μl (sample volume + background volume + dispersion during sampling) at the beginning of the focusing run. Under the conditions used, a focused peak volume of about 0.05 μl (peak width ca. 1 mm, detection capillary cross-section 0.05 mm^2) is obtained. Thus, the analyte concentration in the detector is about 20× higher than at the beginning of separation run.

From the Eq. (8), the corrected theoretical resolution was calculated. Their comparison with experimental values, $R_s(n,n+1)_{exp}$, is presented in Table 1. The experimental resolution is comparable with the corrected theoretical one. The resolutions of derivatized PEGs are smaller than that of the oligomaltoses as can be expected on the basis of smaller differences in mobilities between the derivatized PEGs.

4.3. Influence of the composition of leading and terminating electrolytes

The analyses of the model mixture of derivatized PEGs with different leading and terminating ions were carried out. The examples of these analyses are in Fig. 5. The comparison between the two analyses differing in the type of terminating electrolyte are presented in Fig. 5a. It is obvious that the composition of terminating electrolyte did not influence the separation pattern. For further study the pH and mobility in the terminating zone was calculated by Becker's procedure [33] modified for PC use. The calculated values of pH for terminating electrolytes in Fig. 5a are very close and the only difference is in their mobilities. The lower mobility of the terminating electrolyte zone increases the span of the mobility gradient. A broader mobility span is counterbalanced by larger total voltage needed for the separation. The ratio of conductivity of terminating zones in Fig. 5a 1 (CHES) and 2 (OH^-) was 2.6.

In the second example, the same terminating electrolytes in combination with different leading electrolytes were used. The leading electrolytes had the same pH and differed only in the type of the leader. In the records 1 and 2 in Fig. 5b, the leaders were choride and HIBA, respectively. The analysis

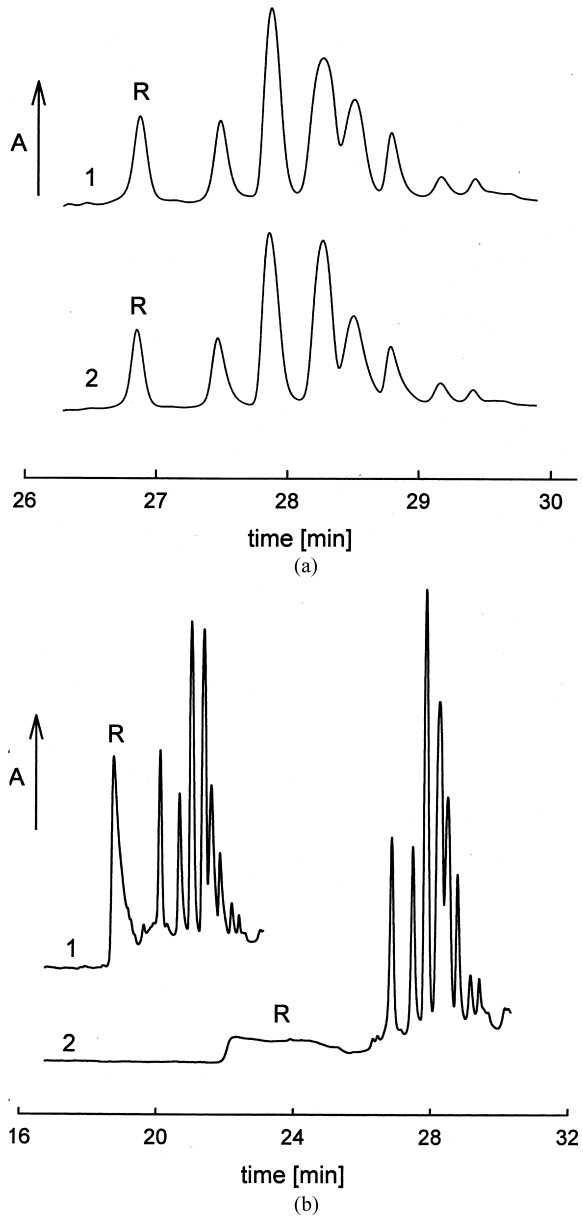

Fig. 5. a: Influence of composition of terminating ion: leading electrolyte 10 m*M* HIBA, 11 m*M* Tris, terminating electrolyte in 1, 50 m*M* CHES, 5 m*M* NaOH, in 2, 0.1 *M* AMP. b: Influence of the leading electrolyte anion: 1–10 m*M* Tris·HCl, 1 m*M* Tris, 2, as 1 in Fig. 5a. Terminating electrolyte 50 m*M* CHES, 5 m*M* NaOH. In all cases 0.06% (w/v) HPMC, 5 μg/ml PEI were added to the leading electrolyte, background 4% Ampholine pH 3.5–10.0, sample volume 500 nl, background volume 400 nl, $I=12$ μA, $\lambda=270$ nm. *R* represents the peak of reagent.

with chloride is faster than with HIBA by approximately 25% which corresponds to the ratio of leading ions transfer numbers in the electrolytes compared. As expected, the mobility of the leading electrolyte determines the span of the mobility gradient. The peak of the reagent in the case of analysis with HIBA is not focused. Its mobility is higher than that of the leading electrolyte and that is why the reagent moved in the zone electrophoretic mode. The width of that zone corresponded to the length of the injected sample plug.

The composition of leading electrolyte influences the concentration in all other zones and due to this also the profile of the conductivity gradient. The change in the profile of the conductivity gradient caused a change in the separation.

4.4. Influence of injected amount of carrier ampholytes

From the theory [16], it follows that the resolution increases with the square root of the length of the conductivity gradient. When the composition of the leading electrolyte does not change, the conductivity gradient length is approximately a linear function of the amount of carrier ampholytes. According to this, the resolution increases with an increasing amount of carrier ampholytes up to some maximum. It corresponds to the maximum amount of carrier ampholytes that can be still focused towards the steady state. Further addition of carrier ampholytes causes the decrease of resolution because the zones do not reach the steady state, see also Ref. [19]. The optimal amount of carrier ampholytes was 24 μg under conditions as in Fig. 2b.

4.5. Influence of electric current

The dependence of resolution on electric current for derivatized oligomaltoses was examined. The resolution increased with increasing electric current until the plateau was reached. In this part of the dependence the resolution changed only slightly. Then the resolution decrease was indicated. The initial increase of resolution is in agreement with Eq. (4). The decrease can be explained by the overheating by developed Joule heat. Under conditions as in Fig. 2b the optimal electric current obtained was 12 μA.

5. Conclusions

The separation and focusing of derivatized polyethylene glycols and oligomaltoses performed are in qualitative agreement with the theory of focusing of strong electrolytes in the conductivity gradient [16]. The increase in analyte concentration by more than one order of magnitude occurs during the separation run. Since the conductivity gradient was generated by ITP migration of carrier ampholytes, its shape is influenced by the pH of the leading electrolyte. Consequently, leading electrolytes in limited pH range gave useful conductivity gradients. To avoid this, it was suggested [34] to generate the conductivity gradient by stacking of a series of strong electrolytes. However, a suitable background based on strong electrolytes has still to be synthesized. In future, the possibilities for the generation of the conductivity gradient consisting of strong electrolytes will be studied.

Acknowledgements

This work was supported by a grant of the Academy of Sciences of the Czech Republic No. A 4031504.

References

[1] F.M. Everaerts, J.L. Beckers, Th.P.E.M. Verheggen, Isotachophoresis, Elsevier, Amsterdam, 1976.
[2] P. Boček, M. Deml, P.Gebauer, V. Dolník, Analytical Isotachophoresis, VCH, Weinheim, 1988.
[3] F. Acevedo, J. Chromatogr. 545 (1991) 391.
[4] F. Acevedo, Electrophoresis 14 (1993) 1019.
[5] L. Křivánková, P. Gebauer, P. Boček, J. Chromatogr. A. 716 (1995) 35.
[6] T. Manabe, H. Yamamoto, T. Okuyama, Electrophoresis 10 (1989) 172.
[7] H. Yamamoto, T. Manabe, T. Okuyama, J. Chromatogr. 480 (1989) 331.
[8] P. Delmotte, Sci. Tools 24(3) (1977) 33.
[9] F.M. Everaerts, M. Guerts, F.E.P. Mikkers, Th.P.E.M. Verheggen, J. Chromatogr. 119 (1976) 129.

[10] F. Acevedo, J. Chromatogr. 470 (1989) 407.
[11] S. Hjertén, M. Zhu, J. Chromatogr. 387 (1987) 127.
[12] J. Čáslavská, S. Molteni, J. Chmelík, K. Šlais, F. Matulík, J. Chromatogr. A 680 (1994) 549.
[13] T. Izumi, T. Nagahori, T. Okuyama, J. High Resolut. Chromatogr. 14 (1991) 351.
[14] R. Charlionet, A. Bringard, Ch. Davrinche, M. Fontaine, Electrophoresis 7 (1986) 558.
[15] A. Bringard, R. Charlionet, Electrophoresis 11 (1990) 802.
[16] K. Šlais, J. Chromatogr. A 764 (1997) 309.
[17] H. Svensson, Acta Chem. Scand. 15 (1961) 325.
[18] M. Št'astná, V. Kahle, K. Šlais, J. Chromatogr. A 730 (1996) 261.
[19] M. Št'astná, K. Šlais, J. Chromatogr. A 768 (1997) 283.
[20] J.W. Jorgenson, K.D. Lukacs, Anal. Chem. 53 (1981) 1298.
[21] F. Foret, M. Deml, P. Boček, J. Chromatogr. 452 (1988) 601.
[22] F. Foret, M. Deml, V. Kahle, P. Boček, Electrophoresis 7 (1986) 430.
[23] K. Šlais, Z. Friedl, J. Chromatogr. A 661 (1994) 249.
[24] K. Šlais, Z. Friedl, J. Chromatogr. A 695 (1995) 113.
[25] J.C. Reijenga, G.V.A. Aben, Th.P.E.M. Verheggen, F.M. Everaerts, J. Chromatogr. 260 (1983) 241.
[26] Th.P.E.M. Verheggen, A.C. Schoots, F.M. Everaerts, J. Chromatogr. 503 (1990) 245.
[27] Th.P.E.M. Verheggen, F.M. Everaerts, J. Chromatogr. 638 (1993) 147.
[28] J.K. Towns, F.E. Regnier, J. Chromatogr. 516 (1990) 69.
[29] P. Jackson, Biochem. J. 270 (1990) 705.
[30] P. Jackson, G.R. Williams, Electrophoresis 12 (1991) 94.
[31] S. Hjertén, J. Chromatogr. 347 (1985) 191.
[32] J.C. Sternberg, Adv. Chromatogr. 2, 1966.
[33] J.L. Becker, F.M. Everaerts, J. Chromatogr. 68 (1972) 207.
[34] K. Šlais, Presented at HPLC'97, Birmingham, J. Chromatogr. A, submitted for publication.